Effects of an artificial hole on the crystal growth of large grain REBCO superconductor

Hwi-Joo Lee[a], Yi-Seul Hong[a], Soon-dong Park[b], Byung-Hyuk Jun[b], Chan-Joong Kim[b], and Hee-Gyoun Lee[a, *]

[a] *Korea Polytechnic University, Siheung, Korea*
[b] *Korea Atomic Energy Research Institute, Taejon, Korea*

Abstract

This study presents that various grain boundary junctions are prepared by controlling the seed orientation combined with an artificial hole in a melt process REBCO bulk superconductor. Large grain YBCO superconductors have been fabricated with various grain boundary junctions that the angle between the grain boundary and the <001> axis of Y123 crystal is 0°, 30° and 45°, respectively. The presence of the artificial hole is beneficial for the formation of clean grain boundary junction and single peak trapped magnetic field profiles have been obtained. Artificial hole makes two growth fronts meet at a point on a periphery of the artificial hole. The presence of artificial hole is not likely to affect on the distribution of Y211 particles. The newly formed <110> facet lines are explained by the formation of new Y123/liquid interface with (010) crystallographic plane.

Keywords: REBCO, grain boundary junction, crystal growth, artificial hole, facet line

1. INTRODUCTION

High magnetization high Tc REBCO bulk superconductors have been fabricated by a melt process [1] and large grain specimens are prepared by using a top-seed melt growth (TSMG) process. However, TSMG takes a long process time and therefore multi-seed technique has been developed [2-5]. Even though multi-seed technique has a big advantage in reducing a processing time, the weak link grain boundaries are formed because of the presence of the trapped liquid phase at the grain boundary where two growth fronts meet. Several techniques [6-10] have been suggested for obtaining clean grain boundaries with no trapping of un-reacted liquid phase. The control of seed orientation is one of the methods. Shi et al. [11] reported that the grain boundary junction with no weak link was obtained by aligning the <110> axis of two seeds parallel each other and thereby fast growing (110) plane of each seed meet together in the middle of the seeds and pushes out the melt upward and downward resulting in no trapping of liquid phase at the grain junction. Kumar et al. [7] has used a buffer pellet between seed and compact and fabricated a high quality bulk superconductor because the weak link grain junction is formed in the buffer pellet and is not extended to YBCO compact due to a proximity effect. However, both methods are available only when the distance between the seeds is close. Meanwhile, it appears that the two dimensional array of the seeds with 45°-45° boundaries also results in the formation of weak link grain boundary junctions that lead to poor magnetization characteristics of bulk superconductors [12]. Therefore, it is need to develop a method to eliminate the trapping of the liquid phase at the grain boundary junctions formed when two grains meet.

It has been showed that the presence of artificial hole through the compact thickness did not lead to the reduction of the magnetization of large grain bulk superconductor [13-17]. They also showed that the artificial holes give an advantage of the reduction of pores in a sample which leads to enhanced mechanical properties. It has been also demonstrated that the filling of the artificial holes using epoxy or metals can reinforce the bulk materials and enhance the toughness of the bulk superconductor [14-15, 17].

In this work, an artificial hole is provided at the side edge of the compact and seed is placed between artificial hole (Fig. 1) and side wall of the compact. By varying the seed alignment, various grain boundary junctions have been formed at the opposite side of the seed and the characteristics of crystal growth and grain boundary junction have been investigated.

2. EXPERIMENTALS

$Y_{1.5}Ba_2Cu_3O_{7-y}$ (hereafter Y1.5) powder was used as a raw material in this study. Y1.5 powder was made by mixing 1 mole Y123 (Solvay Germany, 99.9 % purity, 2–3 μm in size) with 0.25 mole Y_2O_3 (BM-CHEM HI-TECH Co., Ltd, China, 99.99 % purity, 0.12–3 μm in size) powder. 1 wt. % CeO_2 powder was added to the Y1.5 powder to refine Y211. An appropriate amount of Y1.5 powder was put into a steel mold with a diameter of 40 mm. Vertical artificial holes with a diameter of 5 mm were drilled through the thickness 5 mm apart from the side wall of the

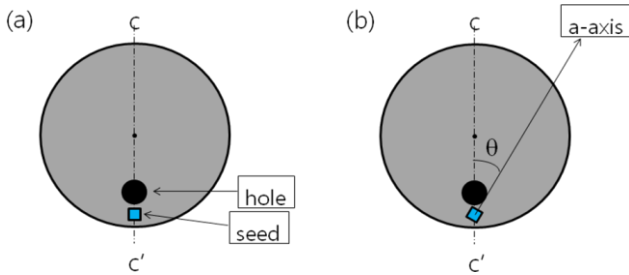* Corresponding author: hglee@kpu.ac.kr

Fig. 1. (a) a schematic drawing that shows the position of the artificial hole and the Sm123 seed. (b) an angle between the center line and the a-axis of seed crystal.

compacts. Before drilling, cold isostatic pressing was conducted for further densification of the compacts.

Fig. 1(a) depicts a schematic that shows the position of the artificial hole and the Sm123 seed. Fig. 1(b) shows how the seed orientation was varied in order to control the grain boundary junction. By changing the angle (θ) between the a-axis of seeds and the line connecting the centers of the compact and the artificial hole, various grain boundary junctions were able to obtain. Line c-c' connects the centers of the compact and the artificial hole. The seed center was tried to locate on the line c-c' at our best. The angle, θ, was chosen as to be. For convenience, we present then as 0-0 boundary, 30-30 boundary and 45-45 boundary when the angle, θ, is 0°, 30° and 45°, respectively.

The heat treatment procedure for melt growth (MG) was similar to those reported in the literature [18]. The cooling rate controlled with 0.25℃h^{-1} at the temperature regime for the growth of Y123 grains. After the MG heat treatment, Y1.5 samples were heated to 500℃ at a rate of 200℃h^{-1} in flowing oxygen for oxygenation, held at this temperature for 50 h, cooled to 400–500℃ at a rate of 100℃h^{-1}, held at this temperature for 200-300 h, and then cooled to room temperature at a rate of 200℃h^{-1}.

Trapped magnetic fields at 77 K were measured for the top surface and the cross section of the field-cooled samples. A trapped magnetic field (B) measurement was performed on field-cooled samples. Permanent magnet with a diameter of 30 mm and a surface field of 4.9 kG was placed on the sample, and liquid nitrogen was poured thereon to cool the sample to 77K (field cooling, FC). When the temperature of the sample reached 77 K, the permanent magnets placed on the superconductor were removed, and the magnetic force trapped in the superconductor was measured on the top surface using a hall probe. Microstructures have been investigated using an optical microscope.

3. RESULTS AND DISCUSSION

Fig. 2 shows the schematics showing the idea how various grain boundary junctions are formed with an angle, θ, formed between the <100> axis of seed and the line c-c'

which connects the centers of the artificial hole and the compact. It illustrates the crystal growth scenario and the procedures how 0-0, 30-30, and 45-45 grain boundary junctions are formed. The numbers in the drawings denotes the sequence of the crystal growth procedure. Fig. 2(a) shows the process how 0-0 grain boundary junction is formed. Two growth fronts with $\theta = 0$ meet at the point J and 0-0 grain boundary junction is extended along the red-colored line. <110> facet lines will be formed along the yellow-colored line. The formation of the <110> facet lines is similar with the other works [2-10]. Suggested scenario may be available under the assumption that the crystal growth occurs uniformly in all the directions. Grain boundary junction and <110> facet line may not be straight if there are asymmetric or inhomogeneous nature of the crystal growth due to either chemical and/or geometrical non-uniformities.

Fig. 2(b) shows the process how 30-30 grain boundary junction is formed. In this case, crystal growth behavior is more complex than in the case of the formation of 0-0 grain boundary junction. Crystal will grow to the line 1 and meet at the point, J, on the periphery of an artificial hole. Then, the left Y123/liquid growth interface will form a tangential line with the periphery of an artificial hole. New Y123/liquid interface will be generated once that the crystal grows further than the tangential line. In order to minimize the Y123/liquid interface energy, a new interface will be of a crystallographic plane of (010) if the existing interface is (100) plane. The generation of new (010) plane interface resulted in the formation of <110> facet line as presented as yellow line. As crystal grows further, right side growth sector will meet the same situation as the left growth sector experienced. Therefore, another <110> facet line will formed starting from the point, J', on the periphery of an artificial hole. Two growth sectors will meet in the middle area between two <110> facet lines and forms a grain boundary junction along the line presented as red color. Suggested scenario may be also available under the assumption that the crystal growth occurs uniformly in all the directions.

Fig. 2(c) shows the process how 45-45 grain boundary junction is formed. In this case, crystal growth behavior is nearly the same with the case of the formation of the 30-30 grain boundary junction. As the Y123 crystal grows, crystal reaches line 2 which is a tangential to the periphery of the artificial hole. As the crystal grows further than line 2, new Y123/liquid interface will be formed as the red-colored lines presented in line 3. In order to minimize the Y123/liquid interface energy, new interface with red color will be a crystallographic plane of (010) if the blue-colored original interface is (100) plane. The generation of new (010) plane interface resulted in the formation of <110> facet line. As like shown in Fig. 2(b) and 2(c), there are two tangential lines.

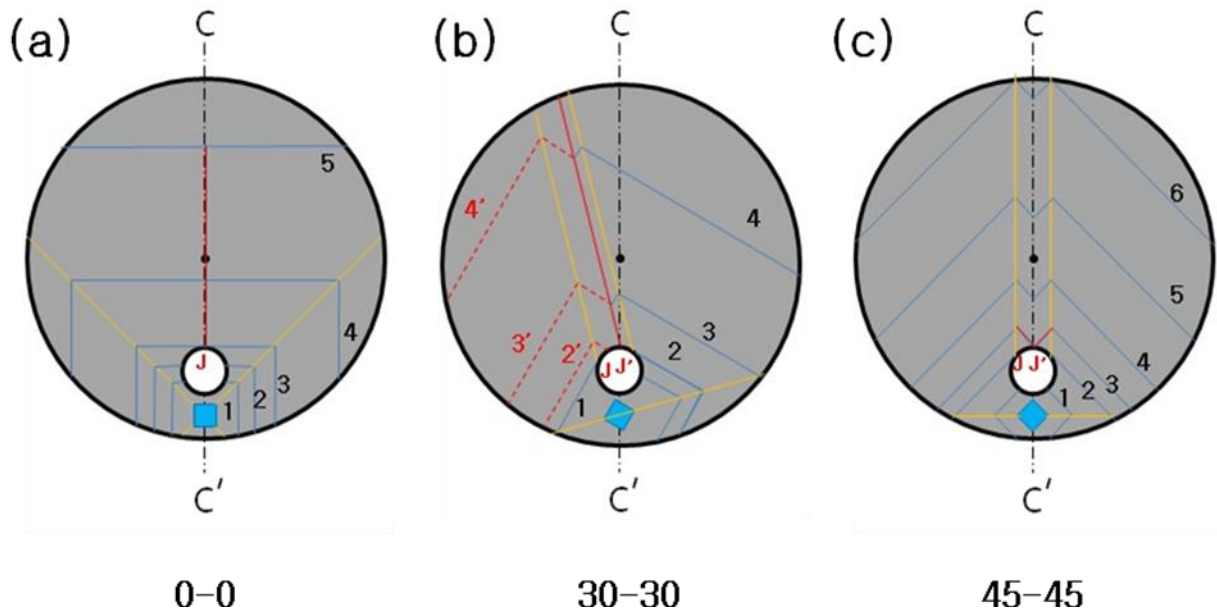Hwi-Joo Lee, Yi-Seul Hong, Soon-dong Park, Byung-Hyuk Jun, Chan-Joong Kim, and Hee-Gyoun Lee

Fig. 2. schematics showing the procedures how various grain boundary junctions are formed. (a) 0-0 grain boundary junction (θ=0°) (b) 30-30 grain boundary junction (θ=30°) (c) 45-45 grain boundary junction (θ=45°). Lines indexed with number shows the crystal growth sequence. Yellow lines represents the <110> facet lines.

Thereby, two new <110> facet lines are formed from both of left side and right. Chaud et al. [13] also have reported the formation of striation in the TSMG specimen with array of artificial holes with a diameter of 1 mm which is much smaller than this work. Two growing interfaces will met in the middle of two growing fronts as the grain growth proceeds further. Crystal growth proceeds from line 2 to line 3 (in Fig. 2(c)), two growing fronts is likely to meet at single point, J, as line 3. Therefore, there is little possibility of liquid trapping at the grain boundary junction which will be formed along the line C-C' with further crystal growth as drawn as lines 4-6(in Fig. 2(c)). It is considered that the artificial hole leads to the formation of clean grain boundary junction as well as the formation dual streaks of <110> facet lines. Single <110> facet line might be formed in upward direction along the C-C' line if the artificial wall was not present.

Fig. 3 shows the top-views of the specimens with 0-0, 30-30, and 45-45 grain boundary junction, respectively. It is seen that the grain shape and <110> facet line are varied depending on the change of the angle, θ, of Fig. 1(b). It is evident that <110> facet lines are not quite straight as reported in the literatures [2,5,15] and rather bent. Four-fold <110> facet lines are closely related to the four-fold crystallographic structure of REBCO crystal and the appearance of four fold-face line represents the epitaxial growth of seed without the nucleation of subsidiary grains [2,5]. The <110> facet lines are the lines where the a-axis growth sector and the b-axis growth sector meet together. There is no reason of asymmetric growth between a-axis growth sector and b-axis growth sector as far as the compact is symmetric and seed is placed at compact center. Therefore, the bent <110> facet line means

that the competition between a-axis growth sector and b-axis growth sector is present because somewhat asymmetry parameters exist. The <110> facet line will be bend toward the direction of the growth sector with weak driving force of crystal growth from the growth sector with weak driving force of crystal growth. More fundamentally, the bending of the <110> facet line may be the outcome of the difference of growth rate in <110> crystallographic directions. There are two possible reasons evolving the different growth rate;

(a) Variation of chemical composition
(b) Asymmetry of mechanical force

Firstly, the mechanical force may arise from the volume contraction during the solidification melt to Y123 crystal and therefore a pulling force will be exerted to the crystal growth fronts. Tensile force acting on the growth front may possibly affect on the deformation of crystal shape [19] and thereby might result in the formation of curved <110> facet lines. Secondly, the geometrical asymmetry may rdisturb the uniform diffusion of the atomic elements of Y, Ba, and Cu. For instance, the distance between the <110> facet lines becomes closer with the crystal growth and the diffusion is the direction normal to the facet lines become slower. Therefore, a-axis sector and b-axis sector may have dissimilar melt interface with different chemical compositions which result in the different growth rate.

Comparing the suggested growth models in Fig. 2 and the melt processed specimens in Fig. 3, it can be said that the crystal shapes, the generation of the <110> facet lines and the formation of grain boundary junction are well coincided with the predictions explained previously in Fig.

Fig. 4. Optical image of the top surface the specimen with 30-30 grain boundary junction.
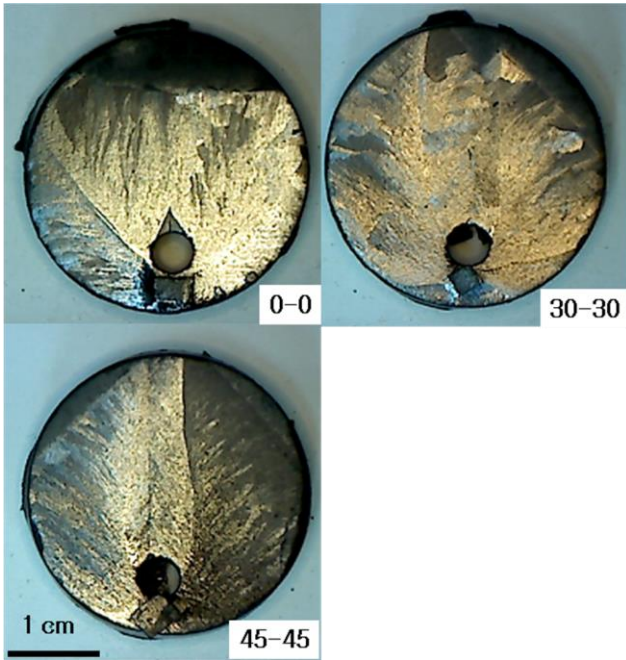
Fig. 3. Optical images of the top surface of the specimens with 0-0, 30-30, and 45-45 grain boundary junction, respectively. Digital images clearly shows the <110> facet lines and the growth fronts. However, the grain boundary junctions are not clear.

2(a) and Fig. 2(c) for 0-0 and 45-45 specimens, respectively. However, the crystal growth features of the 30-30 specimen are not matched with the suggested structures in Fig. 2(b).

Fig. 4 shows surface view of another specimen with 30-30 grain boundary junction. It is seen that the macrostructure of another 30-30 specimen is well matched with the structures suggested in Fig. 2(b). It is also seen that the <110> facet lines and the grain boundary junction are curved. Lines are drawn in the picture for ease of eye guidance (dotted line for the <110> facet lines and a middle line for the grain boundary junction). Chaud et al. [13] reported that their TSMG specimen with many artificial holes with a diameter of 1 mm observed the streaks that were formed by the recombination of the a-axis growth sector and the b-axis growth sector. Their results show that the presence of these streaks (grain boundary junctions) rather leads to the increase of the trapping magnetic field of the specimens [13, 15]. The prediction about the effects of an artificial hole, which was made in Fig. 2, clearly explains the formation of the <110> facet lines and various grain boundary junctions with different angle, θ, in Fig. 1(b).

Fig. 5 shows the trapped magnetic field of the specimen with 0-0 grain boundary junction. It is seen that 0-0 junction specimen show no characteristics of weak link grain boundary junction. There is no drop of magnetic trapping force where 0-0 grain boundary junction is supposed to be present.
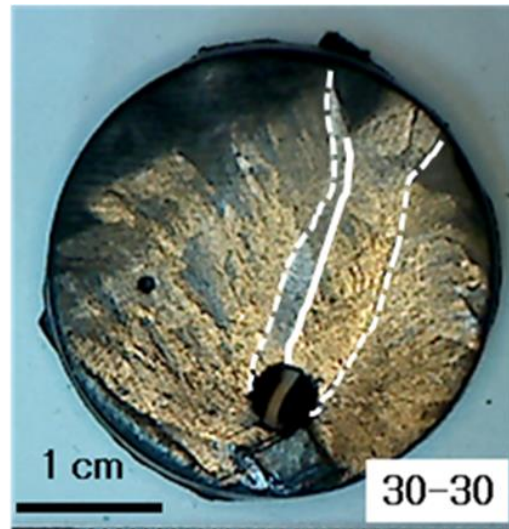
Fig. 6 shows the trapped magnetic field of the specimen with 30-30 grain boundary junction. It is seen that two contour line map is not symmetrical but is well matched with the grain shape. It is also considered that there is no evidence of the presence of the weak link grain boundary junction.

Fig. 7 shows the trapped magnetic field of the specimen with 45-45 grain boundary junction. It is seen that two contour line map is not symmetrical but is well matched with the grain shape. It shows that there is a valley. It can be thought that the appearance of a valley is indication of the presence of the weak link grain boundary junction.
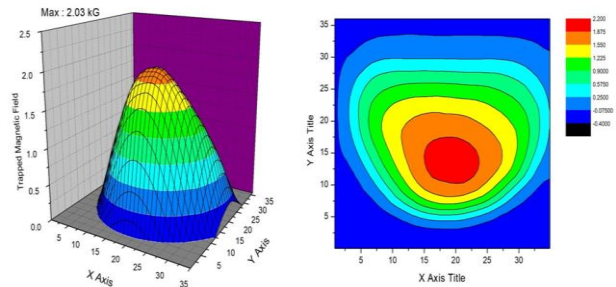

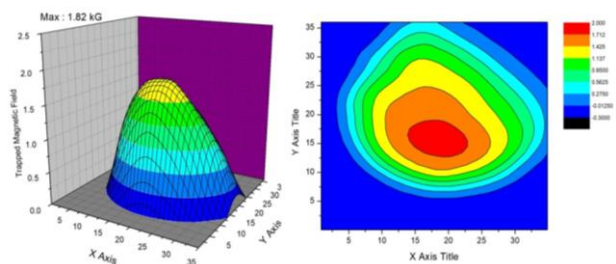Fig. 5. Trapped magnetic field of the specimen with 0-0 grain boundary junction.

Fig. 6 Trapped magnetic field of the specimen with 30-30 grain boundary junction.

Hwi-Joo Lee, Yi-Seul Hong, Soon-dong Park, Byung-Hyuk Jun, Chan-Joong Kim, and Hee-Gyoun Lee
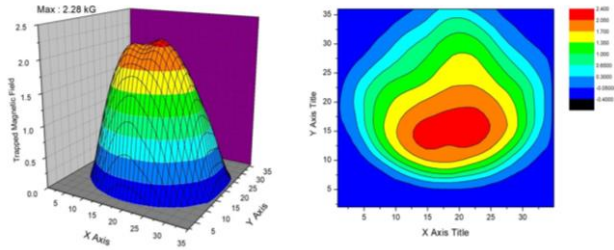

Fig. 7. Trapped magnetic field of the specimen with 45-45 grain boundary junction.

From the observations about the trapped magnetic field profiles from Figs. 5 - Fig. 7, it can be said that all the grain boundary junctions of 0-0, 30-30 and 45-45 junction shows the behavior of clean grain boundary without the entrapping of the un-reacted liquid phase even though the 45-45 specimen shows a valley in the trapped magnetic field curve. Due to the circular geometric characteristics of artificial hole, the Y123/liquid interfaces move along the periphery of the artificial hole from two opposite directions and two growth fronts always meet at single point on the periphery of the circular artificial hole. Thereafter, the growth competition in <110> direction between two growth fronts has occurred and there is little opportunity of liquid trapping at the grain boundary. From this geometrical reason, it is more likely that the appearance of valley for 45-45 specimen may have other reason than the trapping of liquid phase in grain boundary junction. There are many attempts [19-24] to eliminate the weak link nature of the grain boundary junctions in the REBCO bulk superconductor which have been prepared by multi-seeded TSMG. It is thought that this study provides an basic idea how to control the characteristics of the grain boundary junctions and the crystal growth behavior by using the artificial hole though the compact thickness.

Fig. 8 shows the low magnification digital optical microscopic image of the specimen with 0-0 grain boundary junction. It is observed that the diameter of artificial hole was reduced from ϕ = 5 mm to ϕ = 4.7 mm after the melt process. We have carefully observed the areas near the grain boundary junction for all the specimens with 0-0, 30-30 and 45-45 boundaries. As reported in [11], it is hard to observe any structural non-uniformities near to the <110> facet lines. It is also difficult to tell the location in the microstructure where the two growth fronts are met; i.e., the grain boundary junctions are relatively clean under microscopic observations.

Fig. 9 shows the high magnification microstructure of the 45-45 specimen near the periphery of an artificial hole. It is seen that fine Y211 particles are uniformly dispersed though the whole area. It can be also said that any meaningful difference of distribution density of Y211 was not prominent even at the very near to the hole. It means that the presence of the artificial hole did not affect on the distribution of Y211 particles which is crucial for the formation of Y123 superconducting phase though a peritectic reaction of Y211 + Liquid phase → Y123.

Fig. 8. Low magnification digital optical microscopic image of the specimen with 0-0 grain boundary junction.
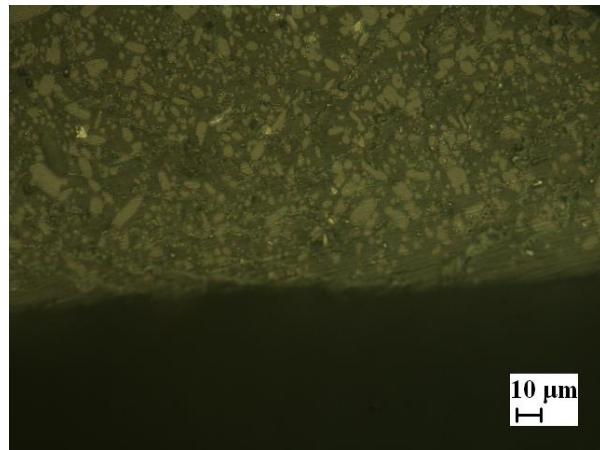

Fig. 9. High magnification microstructure of the 45-45 specimen near the periphery of an artificial hole.

3. CONCLUSIONS

Melt-processed large grain YBCO superconductors with various grain boundary junctions have been successfully prepared by control the seed direction to the grain boundary with the angle of 0°, 30 ° and 45°, respectively. The presence of the artificial hole is beneficial for the formation of clean grain boundary junction and single peak trapping magnetic field profiles have obtained. Artificial hole leads to the formation of new <110> facet lines. The presence of artificial hole is not likely to affect on the distribution of Y211 particles. The newly formed <110> facet lines are explained by the formation of new Y123/liquid interface with (010) crystallographic plane.

REFERENCES

[1] M. Tomita and M. Murakami, "High-temperature superconductor bulk magnets that can trap magnetic fields of over 17 tesla at 29 K," *Nature*, vol. 421, pp. 517-520, 2003.

[2] Y. A. Jee, C-J Kim, T-H Sung and G-W Hong, "Top-seeded melt growth of Y-Ba-Cu-O superconductor with multiseeding." *Supercond. Sci. Technol.*, vol. 13, pp. 195-201, 2000.

[3] C. J. Kim, H. J. Kim, Y. A. Jee, G. W. Hong, J. H. Joo, S. C. Han, Y. H. Han, T. H. Sung, S. J. Kim, "Multiseeding with (100)/(100) grain junctions in top-seeded melt growth processed YBCO superconductors," *Physica C*, vol. 338, pp. 205-212, 2000.

[4] C. J. Kim, G. W. Hong and H. J. Oh, "Multi-seeded melt growth processed YBCO superconductors," *Physica C*, vol. 357-360, pp. 635-641, 2001.

[5] Y. Shi, A. R. Dennis, D. Zhou, D. K. Namburi, K. Y. Huang, J. H. Durrell and D. A. Cardwell, "Factors affecting the growth of multiseeded superconducting single grains*," Cryst. Growth. Des.* 16, pp. 5110-5117, 2016.

[6] D. K. Namburi, Y. Shi, A. R. Dennis, J. H. Durrell and D. A. Cardwell, "A robust seeding technique for the growth of single grain (RE)BCO and (RE)BCO-Ag bulk superconductors," *Supercond. Sci. Technol.*, vol. 31, pp. 044003, 2018.

[7] N. D. Kumar, Y. Shi, W. Zhai, A. R. Dennis, J. H. Durrell and D. A. Cardwell, "Buffer pellets for high-yield, top-seeded melt growth of large grain Y-Ba-Cu-O superconductors," *Cryst. Growth. Des.*, vol. 15, pp. 1472-1480, 2015.

[8] T. Y. Li, C. L. Wang, L. J. Sun, S. B. Yan, L. Cheng, X. Yao, J. Xiong, B. W. Tao, J. Q. Feng, X. Y. Xu, C. S. Li, and D. A. Cardwell "Multiseeded melt growth of bulk Y–Ba–Cu–O using thin film seeds," *J. of Applied Physics*, vol. 108, pp. 023914, 2010.

[9] L. Cheng, L. S Guo, Y. S. Wu, X. Yao and D. A. Cardwell, "Multi-seeded growth of melt processed Gd-Ba-Cu-O bulk superconductors using different arrangements of thin film seeds," *J. of Crystal Growth*, vol. 366, pp. 1-7, 2013.

[10] A. Almalki, D. K. Namburi, M. Ba-Abbad, A. R. Dennis, K. Y. Huang, A. Almutairi, J. H. Durrell and D. A. Cardwell, "Processing and Properties of Bar-Shaped Single-Seeded and Multi-Seeded YBCO Bulk Superconductors by a Top-Seeded Melt Growth Technique," *J. Supercond. Nov. Magn.*, vol. 30, pp. 1397-1403, 2017.

[11] Y. Shi, J. H. Durrell, A. R. Dennis and D. A. Cardwell, "Bulk YBCO seeded with 45°-45° bridge-seeds of different lengths," *Supercond. Sci. Technol.*, vol. 26, pp. 015012, 2013.

[12] C-J Kim, S-D Park, H-W Park and B-H Jun, "Interior seeding for the fabrication of single-grain REBCO bulk superconductors," *Supercond. Sci. Technol.* vol. 29, pp. 034003-034009, 2016.

[13] X. Chaud, S. Meslin, J. Noudem, C. Harnois, L. Porcar, D. Chateigner and R. Tournier, "Isothermal growth of large YBaCuO single domains through an artificial array of holes," *Journal of Crystal Growth*, vol. 275, pp. 855-860, 2005.

[14] J. Noudem, S. Meslin, D. Horvath, , C. Harnois, D. Chateigner, S. Eve, M. Gomina, X. Chaud and M. Murakami, "Fabrication of textured YBCO bulks with artificial holes," *Physica C*, vol. 463-465, pp. 301-307, 2007.

[15] J. Noudem, S. Meslin, D. Horvath, , C. Harnois, D. Chateigner, B. Ouladdiaf , S. Eve, M. Gomina, X. Chaud and M. Murakami, "Infiltration and Top Seed Growth-Textured YBCO Bulks With Multiple Holes," *J. Am. Ceram. Soc.*, vol. 90 [9], pp. 2784–2790, 2007.

[16] K. Yokoyama, R. Igarashi, R. Togasaki and T. Oka, "Pulsed field magnetization characteristics of a holed superconducting bulk magnet," *Physica C*, vol. 518, pp. 117-121, 2015.

[17] K. Yokoyama, K Eranda, Y Zhao, A Katsuki, A Miura and T Oka, "Influence of artificial defects on trapped field performance in a superconducting bulk magnet," *Journal of Physics: Conf. Series*, vol. 871, 012050, pp. 1-5, 2017.

[18] C.-J. Kim, Y.A. Jee, G.-W. Hong, T.-H. Sung, Y.-H. Han, S.-C. Han, S.-J. Kim, W. Bieger, G. Fuchs, "Effects of the seed dimension on the top surface growth mode and the magnetic properties of top-seeded melt growth processed YBCO superconductors," *Physica C*, vol. 331 , pp. 274-284, 2000.

[19] W. Wang, B. Peng, Y. Chen, L. Guo, X. Cui, Q. Rao and X. Yao, "Effective Approach to Prepare Well c-Axis-Oriented YBCO Crystal by Top-Seeded Melt-Growth," *Cryst. Growth Des.*, vol. 14, pp. 2302−2306, 2014

[20] Z. Deng, M. Miki, B. Felder, K. Tsuzuki, N. Shinohara, S. Hara, T. Uetake and M. Izumi, "Influence of grain boundary connectivity on the trapped magnetic flux of multi-seeded bulk superconductors," *Physica C*, vol. 471, pp. 504-508, 2010.

[21] Y. H. Shi, A. R. Dennis, N. H. Babu, C.E. Mancini and D. A. Cardwell, "Properties of grain boundaries in bulk, melt processed Y-Ba-Cu-O fabricated using bridge-shaped seeds," *Supercond. Sci. Technol.*, vol. 25, pp. 045006, 2012.

[22] T. D. Withnell, N. H. Babu, K. Iida, Y. Shi, D. A. Cardwell, S. Haindl, F. Hengstberger and H. W. Weber, "The effect of seed orientation and separation on the field trapping properties of multi-seeded, melt processed Y-Ba-Cu-O," *Physica C*, vol. 445–448, pp. 382–386, 2006.

[23] M. D. Ainslie, J. Zou, H. Mochizuki, H. Fujishiro, Y. Shi, A. R. Dennis and D. A. Cardwell, "Pulsed field magnetization of 0°-0° and 45°-45° bridge-seeded Y-Ba-Cu-O bulk superconductors," *Supercond. Sci. Technol.*, vol. 28, pp. 125002, 2015.

[24] H. Xiang, W. Wang, H. C. Li, X. X. Cui, W. S. Fan, L. S. Guo, X. Yao, Z. Q. Zou and J. Xiong, "Film thermal stability correlation with seeding modes in the growth of $YBa_2Cu_3O_{7-\delta}$ crystals," *J. Appl. Cryst.*, vol. 49, pp. 873–879, 2016.

[25] S. B. Yan, L. J. Sun, T. Y. Li, L. Cheng and X. Yao, "Differences in the thermal stability of $REBa_2Cu_3O_{7-x}$ (RE=Y, Nd) thin films investigated by high temperature in situ observation and melt-texture growth," *Supercond. Sci. Technol.*, vol. 24, pp. 075007, 2011.